IEEE Photonics Journal
An IEEE Photonics Society Publication

Open Access

Design of a Single Nanoparticle Trapping Device Based on Bow-Tie-Shaped Photonic Crystal Nanobeam Cavities

Volume 11, Number 3, June 2019

Yan Gao
Yaocheng Shi, ***Member, IEEE***

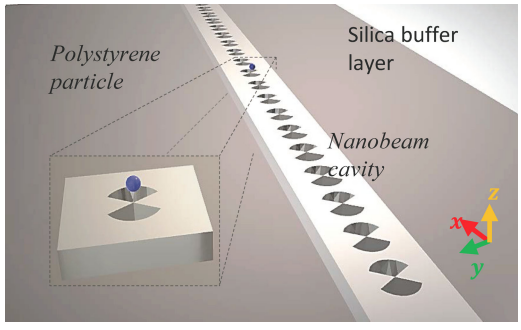

DOI: 10.1109/JPHOT.2019.2911291
1943-0655 © 2019 IEEE

IEEE photonics SOCIETY

IEEE

Design of a Single Nanoparticle Trapping Device Based on Bow-Tie-Shaped Photonic Crystal Nanobeam Cavities

Yan Gao[1,2] **and Yaocheng Shi**[1,2] ***Member, IEEE***

[1]Centre for Optical and Electromagnetic Research, State Key Laboratory of Modern Optical Instrumentation, Zhejiang University, Hangzhou 310058, China
[2]Ningbo Research Institute, Zhejiang University, Ningbo 315100, China

DOI:10.1109/JPHOT.2019.2911291

Manuscript received January 24, 2019; revised April 1, 2019; accepted April 9, 2019. Date of publication April 19, 2019; date of current version May 3, 2019. This work was supported by the National Natural Science Foundation of China under Grant 61675178. Corresponding author: Yaocheng Shi (e-mail: yaocheng@zju.edu.cn).

Abstract: Photonic crystal (PhC) cavities have been widely utilized for the optical trapping. However, it is still challenging to achieve high-efficiency optical trapping of ultrasmall nanoparticles. In this paper, we show optical trapping of a 3 nm size single nanoparticle by using an ultrahigh *Q/V* bow-tie-shaped PhC nanobeam cavity. For the trapping of a single polystyrene nanoparticle with the radius as small as 3 nm, a maximum trapping force of 1.2×10^5 pN/mW is theoretically obtained, which is at least one order of magnitude higher than the previous results. Furthermore, the calculated sensitivity for the cavity is around 350 nm/RIU, which provides a valid solution for monitoring the trapping process of the nanoparticles with ultrasmall size. We believe that such structure with characteristics of extreme light confinement and high trapping efficiency will be conducive to the development of multifunctional on-chip trapping devices.

Index Terms: Integrated optics devices, nanophotonics and photonic crystals, optical tweezers or optical manipulation, laser trapping, photonic crystals.

1. Introduction

Optical trapping or manipulation provide a promising all-optical technology to investigate the light-matter interactions in both physics and biochemistry fields. Nanoparticles such as DNA, proteins and other biological macromolecules with the size ranging from a few nanometers to several micrometers can be manipulated. Ashkin *et al*. firstly demonstrated the optical tweezers through particle trapping experiments under high-focus laser beam [1]. This handling system has been widely used in the trapping substances with dimensions deep down to sub-wavelength scale or even individual atoms [2], [3]. Trapping and enhancing 2D materials is also a potential application [4]. However, the massive and delicate lens system with a high input power are always required, which make it costly and inefficient. Recently, Kawata *et al*. proposed the concept of using near field evanescent waves to achieve a miniature and low power consumption optical trapping and transportation [5], [6].

In order to achieve efficient nanoparticle trapping with lower input power, strong spatial electric field gradient and high amplitude amplification are required. Various near-field devices have been developed, such as nanofibers [7], [8], solid or slotted waveguides [9]–[11], PhC waveguides [11], [13], plasmonic tweezers [14]–[16], whispering gallery mode (WGM) microsphere cavities [17],

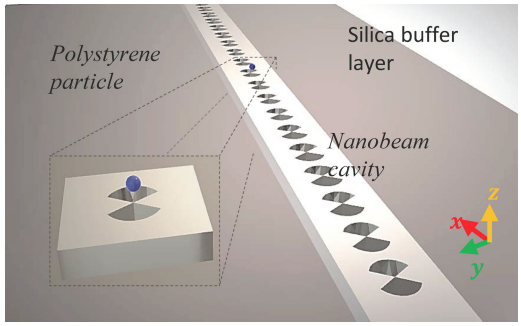

Fig. 1. Schematic of the single nanoparticle trapping device. In this study, a bow-tie shaped nanobeam cavity was well designed to achieve high optical trapping performance.

[18], microring resonators [19] and PhC cavities [20]–[32]. Due to the high quality factor to mode volume ratio (*Q/V*) and the high efficiency systematic optimize methods [33], [37], PhC cavities, especially the 1D-PhC cavities [25]–[32], provide unique advantages in optical trapping or manipulation technologies. By using a typical waveguide-coupled 1D-PhC cavity, Mandal *et al*. showed that for a 50 nm radius polystyrene (PS) nanoparticle, a theoretical maximum trapping force of 0.70 pN/mW can be obtained [25]. Lin *et al*. theoretically achieved a trapping force as large as 2.3 pN/mW for a 50 nm radius PS nanoparticle by a 1D-PhC cavity with waist design [26]. By utilizing the 1D-PhC nanobeam cavity with quadratic tapers, Han *et al*. theoretically showed a trapping force of 300 pN/mW for a 100 nm radius PS nanoparticle [26]. Recently, based on the slotted 1D-PhC nanobeam cavity, Yang *et al*. designed a single nanoparticle optical trapping device, which can achieve a maximum trapping force as large as 8.2×10^3 pN/mW for a 10 nm radius PS nanoparticle [28].

To achieve a high-efficiency optical trapping of even smaller nanoparticles, the optical resonator should be capable of high energy confinement, strong electric field gradient and also suitable light-particle interaction region. Thus, in this work, we propose a single nanoparticle optical trapping configuration via introducing a bow-tie shaped cell modulation to a 1D-PhC cavity [33], [34]. In our design, the evanescent fields with high intensity and fast attenuation are formed into the tips of the cavity cells, which provides an appropriate spatial distribution of the trapping operation. We theoretically achieve a maximum optical trapping force of 1.2×10^5 pN/mW for trapping a 3 nm radius particle by utilizing a systematic cavity structure, which is at least one order of magnitude higher than the previous results. The estimated trapping potential depth and threshold power of 4.06×10^5 k_BT/mW and 0.025 μW are obtained. We believe that the proposed bow-tie shaped nanobeam cavity will provide a precise, efficient way to the compact optical manipulation platform.

2. Structure Design

The schematic of the proposed bow-tie shaped PhC nanobeam cavity designed for single nanoparticle trapping is shown in Fig. 1. The silicon-on-insulator (SOI) platform with a 220 nm silicon core layer and a 2 μm silica insulating layer is considered in our work. The refractive index of the silicon core and the silica buffer are taken as 3.476 and 1.45, respectively. The upper cladding is set to be air with a refractive index of 1.0. The suspended structure is considered in our work to achieve a symmetric configuration which leads to a higher Q factor. The PS particle with refractive index of 1.59 is put near the tip of the central unit of the cavity.

The proposed PhC nanobeam cavity consists of a series of bow-tie shaped etched holes, as shown in Fig. 2(a). The cavity includes a taper region consisting of holes with quadratic changed radii and a mirror region consisting of holes with constant radii. Based on the mode matching theory [35], the quadratic taper design can increase the *Q* factor by several orders of magnitude by significantly reducing the radiation losses. Furthermore, mirror regions with high reflectivity are

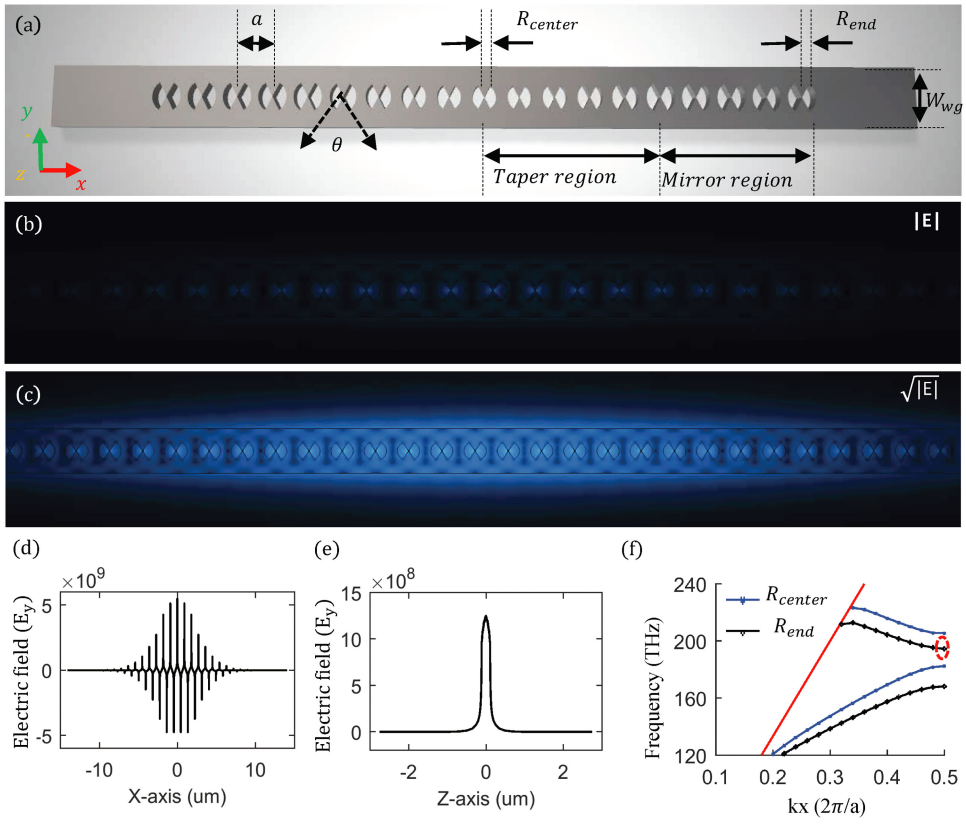

Fig. 2. (a) Schematic of the bow-tie shaped 1D-PhC nanobeam cavity. (b) Simulated fundamental TE-like mode profile ($|E|$) and (c) root number TE-like mode profile ($\sqrt{|E|}$) in x-y section by 3D-FEM method. (d) E_y distribution along X-axis and (e) along Z-axis. (f) Band diagram of the TE-like mode for R_{center} = 150 nm and R_{end} = 180 nm. The red line indicates the light line and the red circle indicates the target cavity resonant frequency of 194 THz.

introduced to enhance the Q factor by decreasing the propagation losses. According to Quan's design scheme [36], the radii for the holes in the taper region are parabolically tapered from R_{center} to R_{end}. The radius of the holes in the taper region is determined by the following formula: $R_i = R_{center} + (i-1)^2(R_{end} - R_{center})/(N_t - 1)^2$, where i is from 1 to N_t, and N_t is the number of holes in the taper region. The radii of the holes in the mirror region are set to a constant R_{end} and the number of holes in the mirror region is N_m.

Fig. 2(b) shows the TE-like fundamental resonant mode ($|E|$) in the x-y plane. From the $\sqrt{|E|}$ distribution shown in Fig. 2(c), we can clearly find the cavity's ability of strong light confinement. In such type of PhC nanobeam cavity, the field distribution is highly concentrated at the tip of the bow-tie shaped holes. Thus, the cavity performance is highly depended on the size of bow-tie center which makes it required higher manufacturing accuracy [37]. Figs. 2(d) and 2(e) show the E_y distribution along X-axis and Z-axis, respectively. The maximum of the electric field locates at the cavity center, which is also set to be the origin of the coordinates. From the figures, one can easily find that the electric field intensity varies dramatically in each cell of the proposed cavity, which provide a significant gradient field distribution preferred by the optical trapping.

The hole radii at the center and the end of the taper region can be determined from the band diagrams. Fig. 2(f) shows the calculated TE band diagram for the PhC cavity with a center hole (blue line) radius R_{center} = 150 nm and an end hole (black line) radius R_{end} = 180 nm. The red line indicates the light line and the red circle indicates the target cavity resonant frequency of 194 THz.

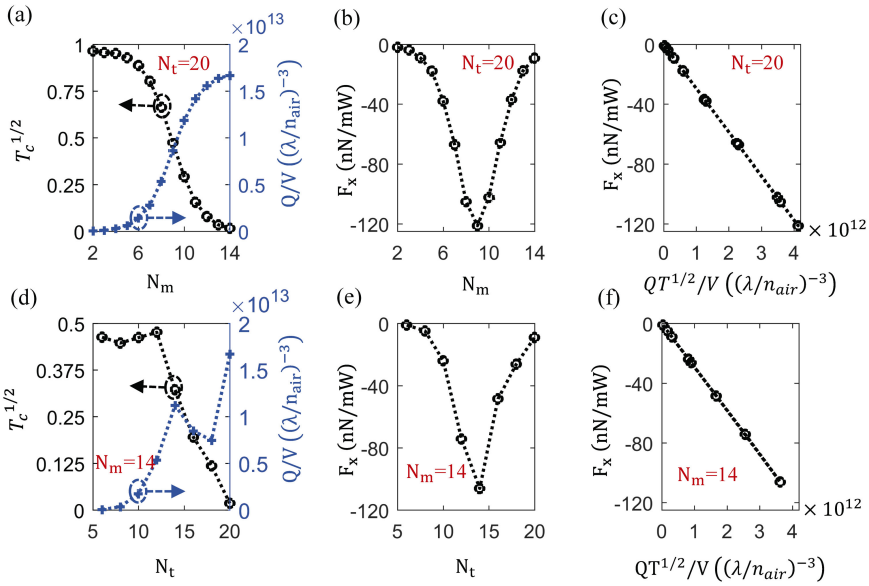

Fig. 3. Influence of the number of the holes N_m and N_t on trapping performance. The PS nanoparticle is set to be at the position of $x = 5$, $y = 0$, $z = 0$. (a), (b), (c) Set $N_t = 20$ and change N_m from 2 to 14. (d), (e), (f) Set $N_m = 14$ and change N_t from 5 to 20. (a), (d) The relationship between $T_c^{1/2}$, Q/V and holes number. (b), (e) The relationship between the normalized optical trapping force F_x and the number of holes. (c), (f) The relationship between F_x and $\sqrt{T_c}\cdot Q/V$.

Here, the width of the waveguide $w_{wg} = 700$ nm, the period length $a = 450$ nm and the angle of silicon tips $\theta = 60°$.

Three-dimensional finite element method (3D-FEM) was used to calculate the optical trapping force for a 3 nm radius PS nanoparticle. The eigenfrequency solver with a scattering boundary is utilized to solve the resonant mode. The theoretical formulation of the trapping force $\boldsymbol{F}_{trap}$ is [11]:

$$\boldsymbol{F}_{trap} = \oint_S (\langle \boldsymbol{T}_M \rangle \cdot \boldsymbol{n})\, d\boldsymbol{S}. \tag{1}$$

The $\langle \boldsymbol{T}_M \rangle$ is the time-independent Maxwell stress tensor and the formulation is:

$$\langle \boldsymbol{T}_M \rangle = \boldsymbol{D}\,\boldsymbol{E}^* + \boldsymbol{H}\,\boldsymbol{B}^* - \frac{1}{2}(\boldsymbol{D}\cdot\boldsymbol{E}^* + \boldsymbol{H}\cdot\boldsymbol{B}^*)\,\boldsymbol{I}. \tag{2}$$

where $\boldsymbol{D}$ is the electric displacement, $\boldsymbol{H}$ is the magnetic field, $\boldsymbol{E}^*$ and $\boldsymbol{B}^*$ are the complex conjugates of electric field and magnetic flux field, and $\boldsymbol{I}$ is the isotropic tensor. Therefore, the total electromagnetic trapping force acting on the PS nanoparticle can be obtained by calculating and integrating the time-independent Maxwell stress tensor over the surface of the nanoparticle.

From the analysis given in the previous work [27], an optimized optical trapping force can be obtained by utilizing the linear relationship between F_x and $\sqrt{T_c}\ Q/V$, where F_x is the horizontal component of the total optical trapping force $\boldsymbol{F}_{trap}$ along the x direction. The transmittance T_c and Q factor can be easily manipulated by changing the number of the holes N_m and N_t. Fig. 3(a) shows the transmittance T_c and the quality factor Q for the cavity with different number of holes N_m. The cavity transmittance T_c decreases with the increases of N_m (with $N_t = 20$) since the reflection intensity on both sides of the cavity increases. However, the Q factor will increase with N_m due to a higher light confinement along the propagation direction. One should note that the taper region between the cavity and the waveguide will not be changed to maintain the radiation losses. The optical trapping force is calculated accordingly and the result is shown in Fig. 3(b). The normalized optical trapping force F_x reaches a maximum of 120.68 nN mW^{-1} at $N_m = 9$ and $T_c = 0.23$. We also calculate the relationship between the normalized optical trapping force F_x and $\sqrt{T_c}\cdot Q/V$. From Fig. 3(c), F_x is

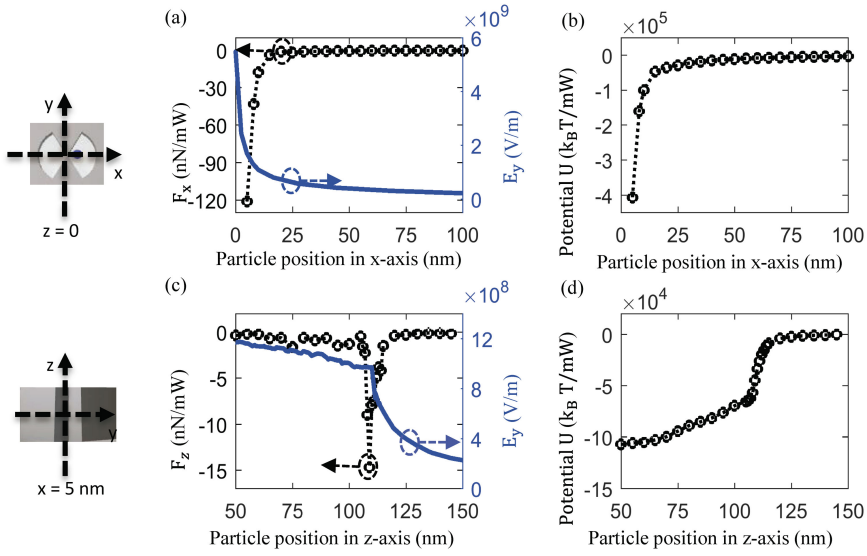

Fig. 4. (a) Evolution of optical trapping force F_x (black curve) and distribution of electric field component E_y (blue curve) when the PS moves along X-axis. (b) Distribution of calculated trapping potential U along X-axis. (c) Evolution of normalized optical trapping force F_x (black curve) and distribution of electric field component E_y (blue curve) when the PS moves along Z-axis. (d) Distribution of calculated trapping potential U along Z-axis. Here, the trapping force and trapping potential are normalized by input power in unit nN/mW and k_BT/mW respectively, where k_B is the Boltzmann constant and T is the room temperature of 300 K.

proportional to $\sqrt{T_c}\cdot Q/V$, the same as the one shown in [27]. The above analysis shows that a compromise between the transmittance T_c and Q/V will result in a higher trapping efficiency. Hence, the holes number $N_m = 9$ and $N_t = 20$ are chosen to achieve an optimized trapping force. The simulated Q factor as high as 2.7×10^8 and mode volume as low as 3.12×10^{-5} $(\lambda/n_{air})^3$ can be obtained. When we change N_t and fix $N_m = 14$, similar optimization results can be obtained, as shown in Fig. 3(e). It is noteworthy that the transmittance T_c and Q/V changed with N_t are not monotonous. That is because when the number of periods in the cavity taper region changes, both the propagation losses and radiation losses of the cavity will be changed, which causes a dual impact on the transmittance T_c and the Q factor.

3. Numerical Results and Discussion

According to the analysis given in Section 2, the detailed parameters of the bow-tie shaped 1D-PhC nanobeam cavity are summarized as follows: $w_{wg} = 700$ nm, $a = 450$ nm, $\theta = 60°$, $R_{center} = 150$ nm, $R_{end} = 180$ nm, $N_t = 20$, and $N_m = 9$. PS nanoparticle with radius of 3 nm is put along X-axis and Z-axis to investigate the trapping characteristics of the optimized cavity. The trapping potential of the PS nanoparticle at a specific position can be obtained by integrating F_x along the corresponding shifting path. Fig. 4(a) shows the component of the normalized trapping force F_x along X-axis. F_x reaches its maximum near the center of the bow-tie shaped 1D-PhC nanobeam cavity (black curve). This is reasonable since the largest gradient of electric field strength occurs over a short distance near this position (blue curve). Considering the size of the PS nanoparticle and the geometry of the cavity, a maximum value of 120.68 nN/mW of the normalized optical trapping force F_x can be achieved. In Fig. 4(c) and Fig. 4(d), the x, y coordinates of the PS nanoparticle are set to the fixed value of $x = 5$, $y = 0$. Along Z-axis, the maximum value of the component of the normalized trapping force along Z-axis F_z occurs at $x = 5$, $y = 0$, $z = 109$, which near the interface between the 1D-PhC nanobeam cavity and the upper cladding. The area of tens of nanometers above the interface also provides a large downward optical trapping force. PS particles moving under Brownian motion in

TABLE 1
Performance of Various on Chip Optical Trapping Device

Trapping System	PS Nanoparticle radius (nm)	Trapping force (pN/mW)	Trapping potential (k_BT/mW)	Threshold power (μW)
Typical 1D-PhC cavity [25]	50	2.3	31.3	320
Waist designed 1D-PhC cavity [26]	50	4.2	51	196
1D-PhC nanobeam cavity [27]	100	330	\	\
Slotted 2D-PhC cavity [35]	25	46	3.77×10^{2}	27
Slotted 1D-PhC cavity [28]	10	8.2×10^{3}	1.15×10^{5}	8.7×10^{-2}
Present work	3	1.21×10^{5}	4.06×10^{5}	2.5×10^{-2}

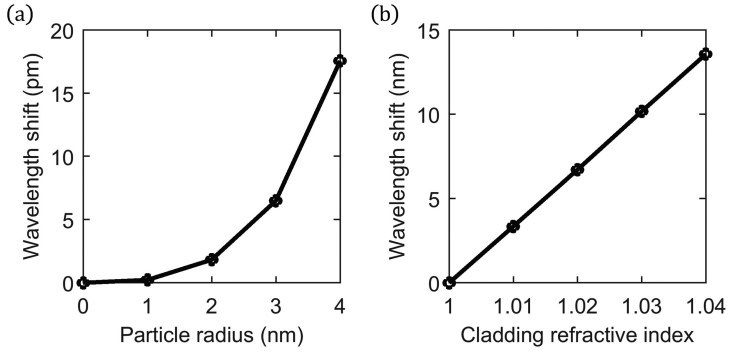

Fig. 5. (a) Resonant wavelength shift with different size of single PS particle, and particle radius of 1, 2, 3, 4 nm is considered. (b) The relationship between the resonant wavelength shift and the refractive index of the cladding.

the upper cladding will first be subjected to a strong downward trapping force and move to the middle area of the bow-tie shaped holes. Then, these PS nanoparticles will move to the bow-tie tip and be trapped by the strong trapping force in the x direction.

Besides the optical force, a large enough trapping potential is also required for a stable trapping. The trapping potential U is calculated by integrating parallel component of trapping force along specific path. Fig. 4(c) and 4(d) show the trapping potential distribution along x and z direction, respectively. The deepest depth of potential (ΔU) reaches 4.06×10^5 k_BT/mW in x direction and 1.07×10^5 k_BT mW^{-1} in z direction. A stable trapping required the depth of trapping potential larger than $10\,k_BT$ [18]. Here, k_B is the Boltzmann constant and T is the system temperature that is set to be room temperature ($T = 300$ K). Thus, an ultra-small threshold power of 0.025 μW that required for stable trapping can be calculated. For the present design with a 1.0 mW input power, the depth of trapping potential in x direction reaches 4.06×10^5 k_BT, which is much deeper than the required depth for stable trapping (10 k_BT). Therefore, we can achieve stable trapping of a 3 nm radius PS nanoparticle in such a low input power (0.025 μW), together with a considerable maximum trapping force (1.21×10^5 pN/mW).

Several different designs of previous work are listed in Table 1 for comparison. From the table, we can find that the present structure provides much higher trapping efficiency and stability for nanoparticle with ultra-small size nanoparticle.

As the development of various optical trapping technologies, nanoparticles with size down to nm can be trapped. However, conventional fluorescent labeling technology cannot work when the particle size is further reduced. Therefore, sensing based particle detection methods are utilized to indirectly observe the optical trapping process [30]. Thus, high sensitivity is required in the optical trapping device. Fig. 5(a) shows the resonant wavelength shift caused by the trapped single nanoparticle. Here, the PS nanoparticle is set at the position of $x = 5$, $y = 0$, $z = 0$. By trapping a

PS nanoparticle with radius of 3 nm, the resonant wavelength shift will reach 6.5 pm. Considering the high Q (narrow linewidth) of the nanobeam cavity, such small amount of wavelength shift can be observed. Fig. 5(b) shows the resonant wavelength shift as a function of the cladding refractive index. A high sensitivity around 350 nm/RIU can be achieved for the present cavity.

4. Conclusion

In summary, a high-performance nanoparticle trapping device has been theoretically investigated via introducing the bow-tie shaped 1D PhC nanobeam cavity. The proposed nanobeam cavity can be capable of simultaneously possessing high energy limitation, strong electric field gradient and suitable light-particle interaction region. Numerical simulations indicate that the proposed bow-tie shaped 1D-PhC nanobeam cavity can efficiently trap a PS nanoparticle with radius down to 3 nm. The maximum trapping force as large as 1.21×10^5 pN/mW and the trapping potential as deep as 4.06×10^5 $k_B T\ mW^{-1}$ at $T = 300$ K can be theoretically achieved. Furthermore, the proposed cavity shows a sensitivity around 350 nm/RIU, which is preferred for the indirect observation of the optical trapping process by monitoring the wavelength shifts due to the trapped particles. Therefore, such trapping device with characteristics of an extreme light concentration, ultra-compact footprint and high trapping efficiency will be conducive to the development of versatile on-chip applications.

References

[1] A. Ashkin, J. M. Dziedzic, J. E. Bjorkholm, and S. Chu, "Observation of a single-beam gradient force optical trap for dielectric particle," *Opt. Lett.*, vol. 11 no. 5, pp. 288–290, Jun. 1986.

[2] A. Ashkin, J. M. Dziedzic, and T. Yamane, "Optical trapping and manipulation of single cells using infrared laser beams," *Nature*, vol. 330, no. 6150, pp. 769–771, Dec. 1987.

[3] P. W. H. Pinkse, T. Fischer, P. Maunz, and G. Rempe, "Trapping an atom with single photons," *Nature*, vol. 404, no. 6776, pp. 365–368, Mar. 2000.

[4] N. Yi, Z. Liu, S. Sun, Q. Song, and S. Xiao, "Mid-infrared tunable magnetic response in graphene-based diabolo nanoantennas," *Carbon*, vol. 94, pp. 501–506, Nov. 2015.

[5] S. Kawata and T. Sugiura, "Movement of micrometer-sized particle in the evanescent field of a laser beam," *Opt. Lett.*, vol. 17, no. 11, pp. 772–774, Jun. 1992.

[6] K. Okamoto and S. Kawata, "Radiation force exerted on subwavelength particle near a nanoaperture," *Phys. Rev. Lett.*, vol. 83, no. 22, pp. 4534–4537, May 1999.

[7] M. J. Morrissey *et al.*, "Spectroscopy, manipulation and trapping of neutral atoms, molecules, and other particle using optical nanofibers: A review," *Sensors*, vol. 13, no. 8, pp. 10449–10481, Aug. 2013.

[8] J. Huang, X. Liu, Y. Zhang, and B. Li, "Optical trapping and orientation of Escherichia coli cells using two tapered fiber probes," *Photon. Res.*, vol. 3, no. 6, pp. 308–312, Dec. 2015.

[9] T. H. Stievater *et al.*, "Modal characterization of nanophotonic waveguides for atom trapping," *Opt. Mater. Exp.*, vol. 6, no. 12, pp. 3826–3837, Dec. 2016.

[10] X. F. Xu *et al.*, "Reconfigurable sorting of nanoparticles on a thermal tuning silicon based optofluidic chip," *IEEE Photon. J.*, vol. 10, no. 1, Feb. 2018, Art. no. 4900107.

[11] A. H. Yang, S. D. Moore, B. S. Schmidt, M. Klug, M. Lipson, and D. Erickson, "Optical manipulation of nanoparticle and biomolecules in sub-wavelength slot waveguides," *Nature*, vol. 457, no. 7225, pp. 71–75, Jan. 2009.

[12] M. G. Scullion, Y. Arita, T. F. Krauss, and K. Dholakia, "Enhancement of optical forces using slow light in a photonic crystal waveguide," *Optica*, vol. 2, no. 9, pp. 816–821, Sep. 2015.

[13] N. D. Gupta and V. Janyani, "Design and analysis of light trapping in thin film GaAs solar cells using 2-D photonic crystal structures at front surface," *IEEE J. Quantum Electron.*, vol. 53, no. 2, pp. 1–9, Feb. 2017.

[14] M. L. Juan, M. Righini, and R. Quidant, "Plasmon nano-optical tweezers," *Nature Photon.*, vol. 5, no. 6, pp. 349–356, May 2011.

[15] J. C. Ndukaife, A. V. Kildishev, A. Nnanna, V. M. Shalaev, S. T.Wreley, and A. Boltasseva, "Long-range and rapid transport of individual nano-objects by a hybrid electrothermoplasmonic nanotweezer," *Nature Nanotechnol.*, vol. 11, no. 1, pp. 53–59, Nov. 2016.

[16] Z. Chen *et al.*, "Blue-detuned optical atom trapping in acompact plasmonic structure," *Photon. Res.*, vol. 5, no. 5, pp. 436–440, Oct. 2017.

[17] S. Arnold, D. Keng, S. I. Shopova, S. Holler, W. Zurawsky, and F. Vollmer, "Whispering gallery mode carousel–a photonic mechanism for enhanced nanoparticle detection in biosensing," *Opt. Exp.*, vol. 17, no. 8, pp. 6230–6238, Apr. 2009.

[18] J. Zhu, Y. Zhong, and H. Liu, "Impact of nanoparticle-induced scattering of an azimuthally propagating mode on the resonance of whispering gallery microcavities," *Photon. Res.*, vol. 5, no. 5, pp. 396–405, Oct. 2017.

[19] S. Y. Lin, E. Schonbrun, and K. Crozier, "Optical manipulation with planar silicon microring resonators," *Nano Lett.*, vol. 10, no. 7, pp. 2408–2411, Jul. 2010.

[20] M. Barth and O. Benson, "Manipulation of dielectric particle using photonic crystal cavities," *Appl. Phys. Lett.*, vol. 89, no. 25, Dec. 2006, Art. no. 253114.
[21] C. A. Mejia, N. Huang, and M. L. Povinelli, "Optical trapping of metaldielectric nanoparticle clusters near photonic crystal microcavities," *Opt. Lett.*, vol. 37, no. 17, pp. 3690–3692, Sep. 2012.
[22] N. Descharmes, U. P. Dharanipathy, Z. Diao, M. Tonin, and R. Houdre, "Observation of backaction and self-induced trapping in a planar hollow photonic crystal cavity," *Phys. Rev. Lett.*, vol. 110, no. 12, Mar. 2013, Art. no. 123601.
[23] A. Nirmal, A. K. K. Kyaw, J. Wang, K. Dev, X. Sun, and H. V. Demir, "Light trapping in inverted organic photovoltaics with nanoimprinted ZnO photonic crystals," *IEEE J. Photovolt.*, vol. 7, no. 2, pp. 545–549, Jan. 2017.
[24] M. Tonin, F. M. Mor, L. Forro, S. Jeney, and R. Houdre, "Thermal fluctuation analysis of singly optically trapped spheres in hollow photonic crystal cavities," *Appl. Phys. Lett.*, vol. 109, no. 24, Dec. 2016, Art. no. 241107.
[25] S. Mandal, X. Serey, and D. Erickson, "Nanomanipulation using silicon photonic crystal resonators," *Nano Lett.*, vol. 10, no. 1, pp. 99–104, Dec. 2010.
[26] P. T. Lin, T. W. Lu, and P. T. Lee, "Photonic crystal waveguide cavity with waist design for efficient trapping and detection of nanoparticle," *Opt. Exp.*, vol. 22, no. 6, pp. 6791–6800, Mar. 2014.
[27] S. Han and Y. Shi, "Systematic analysis of optical gradient force in photonic crystal nanobeam cavities," *Opt. Exp.*, vol. 24, no. 1, pp. 452–458, Jan. 2016.
[28] D. Yang, F. Gao, Q. T. Cao, C. Wang, Y. Ji, and Y. F. Xiao, "Single nanoparticle trapping based on on-chip nanoslotted nanobeam cavities," *Photon. Res.*, vol. 6, no. 2, pp. 99–108, Feb. 2018.
[29] F. Liang, Y. Guo, S. Hou, and Q. Quan, "Photonic-plasmonic hybrid single-molecule nanosensor measures the effect of fluorescent labels on DNA-protein dynamics," *Sci. Adv.*, vol. 3, no. 5, May 2017, Art. no. e1602991.
[30] F. Liang and Q. Quan, "Detecting single gold nanoparticle (1.8 nm) with ultrahigh-q air mode photonic crystal nanobeam cavities," *ACS Photon.*, vol. 2, no. 12, pp. 1692–1697, Nov. 2015.
[31] H. Du, X. Zhang, J. Deng, Y. Zhao, F. S. Chau, and G. Y. Zhou, "Lateral shearing optical gradient force in coupled nanobeam photonic crystal cavities," *Appl. Phys. Lett.*, vol. 108, no. 17, Apr. 2016, Art. no. 171102.
[32] C. Ciminelli, D. Conteduca, F. DellOlio, and M. N. Armenise, "Design of an optical trapping device based on an ultra-high Q/V resonant structure," *IEEE Photon. J.*, vol. 6, no. 6, Dec. 2014, Art. no. 0600916.
[33] S. Hu and M. S. Weiss, "Design of photonic crystal cavities for extreme light concentration," *ACS Photon.*, vol. 3, no. 9, pp. 1647–1653, Mar. 2016.
[34] S. Hu *et al.*, "Experimental realization of deep subwavelength confinement in dielectric optical resonators," *Sci. Adv.*, vol. 4, no. 8, Aug. 2018, Art. no. eaat2355.
[35] J. Ma, L. J. Martínez, and M. L. Povinelli, "Optical trapping via guided resonance modes in a Slot-Suzuki-phase photonic crystal lattice," *Opt. Exp.*, vol. 20, no. 6, pp. 6816–6824, Mar. 2012.
[36] Q. Quan and M. Loncar, "Deterministic design of wavelength scale, ultra-high q photonic crystal nanobeam cavities," *Opt. Exp.*, vol. 19, no. 19, pp. 18529–18542, Sep. 2011.
[37] F. Wang, R. E. Christiansen, Y. Yu, J. Mørk, and O. Sigmund, "Maximizing the quality factor to mode volume ratio for ultra-small photonic crystal cavities," *Appl. Phys. Lett.*, vol. 113, no. 24, Dec. 2018, Art. no. 241101.